Progress In Electromagnetics Research B, Vol. 9, 105–116, 2008

ON MEASURING THE PERMITTIVITY TENSOR OF AN ANISOTROPIC MATERIAL FROM THE TRANSMISSION COEFFICIENTS

C. A. Valagiannopoulos

Microwaves and Fiber Optics Laboratory
School of Electrical and Computer Engineering
National Technical University of Athens
Heroon Polytechniou 9, GR-15773 Zografou, Athens, Greece

Abstract—The permittivity tensor of an anisotropic material can be predicted with use of the presented technique. A slab of this substance possessing infinitesimal thickness is illuminated by a normally incident plane wave and rigorous expressions for the transmission coefficients are obtained. The derived formulas are linearly expanded with respect to the small thickness of the slice, while simple approximations of the material permittivities are produced by measuring the transmission coefficients for suitable polarizations. These simplified expressions provide a physical intuition about the use and the function of the anisotropy parameters which cannot be achieved via more precise but also more complex patterns. Some diagrams of the prediction error with respect to the dielectric constants, the size of the slab and the operating frequency are included and discussed.

1. INTRODUCTION

Anisotropic materials have been extensively analyzed and studied during several decades as they can describe successfully real-world configurations. Additionally, devices incorporating these materials acquire interesting directionally dependent properties, useful in their operation. In [1], metallic patches on anisotropic slabs constitute frequency selective surfaces, while full-wave solution is obtained by determining the dyadic Green's function and applying the method of moments (MoM). Also in [2], the scattering of a radiating strip by an anisotropic cylinder is studied through solving an integral equation with nonsingular kernel and the variations of the device's features with respect to the anisotropy parameters are shown. Additionally,

a set of useful equations describing the scattering from an azimuthally symmetric, radially inhomogeneous anisotropic sphere is presented in [3] where particular attention is given to the discontinuities leading to delta functions. The case of multi-layered biaxial anisotropic configurations has been also examined with the help of FDTD method [4] where the structure is excited by a Gaussian beam. Moreover, a microwave cylindrical cavity with an annular slot in the perfectly conducting walls and an anisotropic dielectric passing through the slot is studied rigorously for the case of hybrid modes diffraction [5].

As anisotropic materials are so widely utilized, accurate methods of estimating and measuring their permeability and permittivity profiles are necessary to be proposed. In [6], the two-dimensional inverse problem for an inhomogeneous biaxial cylinder is thoroughly presented and the material parameters are reconstructed by the knowledge of the scattered field measured outside. Furthermore in [7], the profile reconstruction of an one-dimensional inhomogeneous anisotropic medium is made through closed-form expressions obtained by using Wentzel-Kramers-Brillouin (WKB) approximation. Finally, in [8] a continuously stratified anisotropic slab under oblique incidence is considered and the corresponding inverse scattering problem is solved with help of frequency-domain techniques. In [9], an optimization approach is used to retrieve the constitutive parameters of a slab of general bianisotropic medium from the recorded reflection and transmission data.

In this work, we present a reliable and applicable technique of estimating the dielectric constants of an anisotropic homogeneous material. A thin slice of this substance and a single accurate measurement of the transmission coefficient, suffice to predict the elements of the permittivity tensor with satisfactory precision. We assume a slab with infinite transversal dimensions and small thickness which is illuminated by a normally incident plane wave. The scattered field is calculated through numerical evaluation of exponential matrices. However, closed-form analytical formulas are derived by applying linear approximations with respect to the infinitesimal thickness of the slab. In this way, simple asymptotic expressions for the permittivity profiles of the anisotropic material are produced and explained. The transmission coefficient can be measured successfully because it is determined by the electric field at each point of the entire area, not across a restricted area of the considered region.

2. PROBLEM STATEMENT

Consider a slab (area 1) of thickness W filled with a lossless, magnetically inert and electrically anisotropic material possessing the following relative permittivity tensor

$$\boldsymbol{\varepsilon}_1 = \begin{bmatrix} \varepsilon_{1xx} & \varepsilon_{1xy} & 0 \\ \varepsilon_{1yx} & \varepsilon_{1yy} & 0 \\ 0 & 0 & 1 \end{bmatrix} \tag{1}$$

with real elements. The background medium is vacuum (ε_0, μ_0) and the structure is excited by a plane wave normally incident to the slab. With reference to the Cartesian coordinate system (x, y, z), defined in Fig. 1, the incident electric field is linearly polarized, not possessing a longitudinal (z) component, while its vector forms an angle Φ with x axis. The choice of the axes x and y is arbitrary. The elements of (1) related to z direction, are unitary (diagonal) or equal to zero (off-diagonal) which makes no difference because our approach assumes transverse electromagnetic fields. Moreover, the same form for $\boldsymbol{\varepsilon}_1$ is assumed and adopted by many researchers when examining two-dimensional configurations with directionally dependent properties [10, 11]. We call the regions $z < 0$ and $z > W$ as areas 0 and 2 respectively. The time dependence is harmonic with an $\exp(+j\omega t)$ form, where ω is the circular frequency of the excitation. The notation $k_0 = \omega\sqrt{\varepsilon_0\mu_0}$ is used for the free-space wavenumber.

The purpose of this work is to find approximate expressions for the permittivity parameters of area 1 based on measurements performed outside the slab.

3. MATHEMATICAL FORMULATION

3.1. Rigorous Solution

In this subsection, the plane wave scattering by the anisotropic slab is solved rigorously. The incident field, taken of unitary magnitude with no loss of generality, is given by:

$$\mathbf{E}_{0,\,inc}(z) = (\mathbf{x}\cos\Phi + \mathbf{y}\sin\Phi)\exp(-jk_0 z) \tag{2a}$$

The reflected and transmitted rays into areas 0 and 2 respectively with arbitrary magnitudes and suitable propagation directions possess the following expressions:

$$\mathbf{E}_{0,ref}(z) = (\mathbf{x}R_x + \mathbf{y}R_y)\exp(jk_0 z) \tag{2b}$$

$$\mathbf{E}_2(z) = (\mathbf{x}T_x + \mathbf{y}T_y)\exp(-jk_0(z-W)) \tag{2c}$$

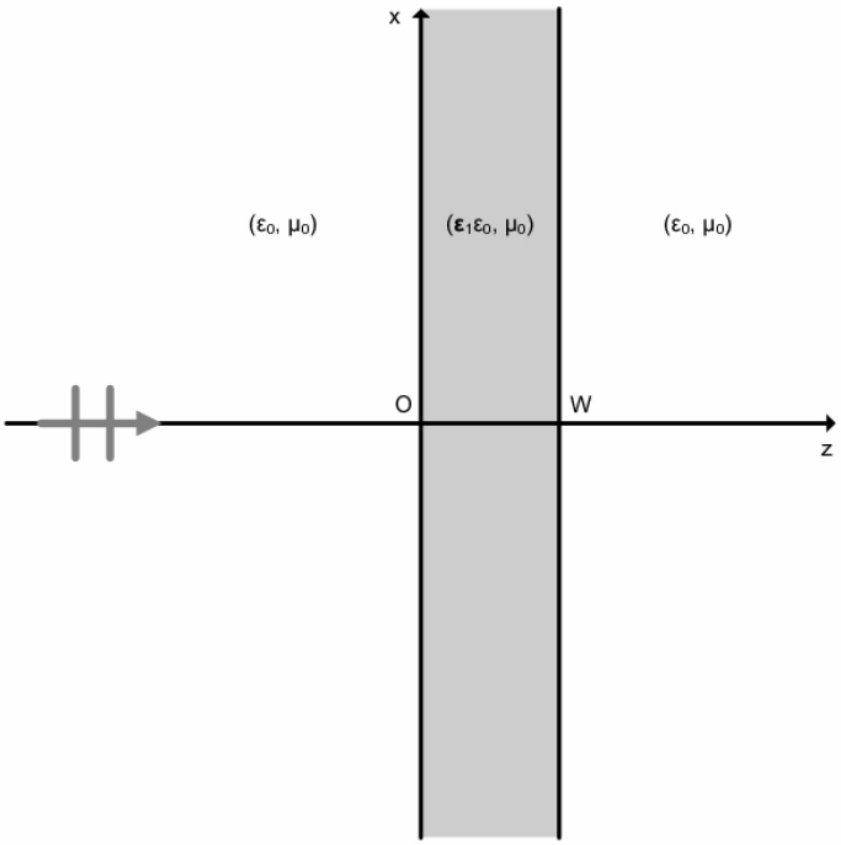

Figure 1. The physical configuration of the investigated structure. An anisotropic slab scatters a plane wave normally incident to it.

The electric field inside the anisotropic slab owns a general form independent from (x, y), due to the symmetry of the structure.

$$\mathbf{E}_1(z) = \mathbf{x}E_{1x}(z) + \mathbf{y}E_{1y}(z) + \mathbf{z}E_{1z}(z) \tag{2d}$$

If one applies the Faraday and Ampere laws to area 1, one notes that $E_{1z}(z) = 0$ and obtains a first-order differential linear system with the solution below:

$$\begin{bmatrix} E'_{1x}(z) \\ E'_{1y}(z) \\ E_{1x}(z) \\ E_{1y}(z) \end{bmatrix} = \mathbf{M}(z) \cdot \begin{bmatrix} E'_{1x}(0) \\ E'_{1y}(0) \\ E_{1x}(0) \\ E_{1y}(0) \end{bmatrix} \tag{3a}$$

where:

$$\mathbf{M}(z) = \exp\{\mathbf{N}z\} = \exp\left\{ \begin{bmatrix} 0 & 0 & -k_0^2\varepsilon_{1xx} & -k_0^2\varepsilon_{1xy} \\ 0 & 0 & -k_0^2\varepsilon_{1yx} & -k_0^2\varepsilon_{1yy} \\ 1 & 0 & 0 & 0 \\ 0 & 1 & 0 & 0 \end{bmatrix} z \right\} \quad (3b)$$

The derivatives with respect to z in (3a), are proportional to the tangential magnetic field in area 1 as the permeability of the anisotropic medium equals μ_0. By enforcing the suitable boundary conditions across the planes $z = 0, W$, a linear system with respect to the reflection and transmission coefficients is derived:

$$\mathbf{A} \cdot \begin{bmatrix} R_x \\ R_y \\ T_x \\ T_y \end{bmatrix} = \mathbf{b} \quad (4a)$$

where:

$$\mathbf{A} = \begin{bmatrix} -jk_0M_{11}(W) - M_{13}(W) & -jk_0M_{12}(W) - M_{14}(W) & -jk_0 & 0 \\ -jk_0M_{21}(W) - M_{23}(W) & -jk_0M_{22}(W) - M_{24}(W) & 0 & -jk_0 \\ -jk_0M_{31}(W) - M_{33}(W) & -jk_0M_{32}(W) - M_{34}(W) & 1 & 0 \\ -jk_0M_{41}(W) - M_{43}(W) & -jk_0M_{42}(W) - M_{44}(W) & 0 & 1 \end{bmatrix} \quad (4b)$$

$$\mathbf{b} = \begin{bmatrix} (M_{13}(W) - jk_0M_{11}(W))\cos\Phi + (M_{14}(W) - jk_0M_{12}(W))\sin\Phi \\ (M_{23}(W) - jk_0M_{21}(W))\cos\Phi + (M_{24}(W) - jk_0M_{22}(W))\sin\Phi \\ (M_{33}(W) - jk_0M_{31}(W))\cos\Phi + (M_{34}(W) - jk_0M_{32}(W))\sin\Phi \\ (M_{43}(W) - jk_0M_{41}(W))\cos\Phi + (M_{44}(W) - jk_0M_{42}(W))\sin\Phi \end{bmatrix} \quad (4c)$$

The notation $M_{\alpha\beta}(z)$ is used for the corresponding (α, β) element of well-conditioned matrix $\mathbf{M}(z)$. The matrix $\mathbf{A}$ of the system is numerically invertible and thus the transmission coefficients of the system (varying with polarization angle Φ) $T_x(\Phi)$, $T_y(\Phi)$ are properly determined.

3.2. Thin Slab Approximation

In this subsection, a simplified approximate solution for the transmission coefficients of the investigated system is derived under the condition that the thickness W of the slab is significantly smaller

than the nonzero elements of matrix $\mathbf{N}$. More specifically, in case $W \to 0$, the following linear approximation for the exponential matrix (3b) is affordable in terms of numerical error:

$$\mathbf{M}(W) \cong \mathbf{I} + \mathbf{N}W \tag{5}$$

where $\mathbf{I}$ is the identity 4×4 matrix. This simplification leads to a linear system similar to (4a)–(4c) which is rigorously solved and yields the following formulas for $T_x(\Phi)$, $T_y(\Phi)$:

$$T_x(\Phi) \cong -2j \frac{\left[\begin{array}{l} k_0W(k_0W-j)^2\varepsilon_{1xy}\sin\Phi + (k_0W(1+\varepsilon_{1yy}+k_0W \\ (-k_0W\varepsilon_{1yx}\varepsilon_{1xy}+\varepsilon_{1xx}(k_0W(1+\varepsilon_{1yy})-2j)))-2j)\cos\Phi \end{array}\right]}{-4+k_0W(k_0W(1+\varepsilon_{1xx}+\varepsilon_{1yy}+\varepsilon_{1xx}\varepsilon_{1yy}-\varepsilon_{1xy}\varepsilon_{1yx})-2j(2+\varepsilon_{1xx}+\varepsilon_{1yy}))} \tag{6a}$$

$$T_y(\Phi) \cong -2j \frac{\left[\begin{array}{l} k_0W(k_0W-j)^2\varepsilon_{1yx}\cos\Phi + (k_0W(1+\varepsilon_{1xx}+k_0W \\ (-k_0W\varepsilon_{1yx}\varepsilon_{1xy}+\varepsilon_{1yy}(k_0W(1+\varepsilon_{1xx})-2j)))-2j)\sin\Phi \end{array}\right]}{-4+k_0W(k_0W(1+\varepsilon_{1xx}+\varepsilon_{1yy}+\varepsilon_{1xx}\varepsilon_{1yy}-\varepsilon_{1xy}\varepsilon_{1yx})-2j(2+\varepsilon_{1xx}+\varepsilon_{1yy}))} \tag{6b}$$

3.3. Formula Inversion

In this subsection, we examine the possibility of determining the permittivity tensor of the anisotropic material through measurements of the transmission coefficients. The choice of infinitesimal slab contributes to this objective as it has three advantages: (I) the formulas of (6a), (6b) are simple, (II) more small-W asymptotic expressions can be obtained and (III) the assumption for a structure with infinite dimensions towards x and y axes can be more easily satisfied for thin slabs. We are not interested for the reflection coefficients as they vanish for $W \to 0$ and it is difficult to separate fields of small magnitudes from an aggregate with substantial values (incident plane wave).

Given the tiny thickness of the anisotropic slice, an additional linear approximation with respect to W is permitted. In particular, we take the first-order Taylor expansion of (6a), (6b) at $W = 0$, in order to produce more functional expressions.

$$T_x(\Phi) \cong \cos\Phi - jk_0W\frac{(1+\varepsilon_{1xx})\cos\Phi + \varepsilon_{1xy}\sin\Phi}{2} \tag{7a}$$

$$T_y(\Phi) \cong \sin\Phi - jk_0W\frac{(1+\varepsilon_{1yy})\sin\Phi + \varepsilon_{1yx}\cos\Phi}{2} \tag{7b}$$

It should be stressed that the real parts of $T_x(\Phi)$, $T_y(\Phi)$ correspond to absent slab ($T_x^2(\Phi) + T_y^2(\Phi) = 1$) and thus are independent from the permittivity parameters. As a result, the measurement procedure should be focused on the imaginary parts of the transmission coefficients which are nonzero even in the case of a real diagonal tensor. Even though they are small, they are easily discernible from the related real parts (waves of opposite phases). The problem arises when the total magnitude of the measured quantity is negligible and that is why we prefer large $T_x(\Phi)$, $T_y(\Phi)$.

When $\Phi = 0$, the x component of the transmission coefficient becomes maximum and simultaneously, the coefficient of ε_{1xy} is vanishing. Therefore, an x-polarized plane wave is suitable for the prediction of the corresponding diagonal element of (1):

$$\varepsilon_{1xx} \cong -1 - \frac{2}{k_0 W}\mathrm{Im}\left[T_x(0)\right] \tag{8a}$$

In the same way, the y component of the transmission coefficient is maximized for $\Phi = \pi/2$ and through it, the following estimation of ε_{1yy} is possible:

$$\varepsilon_{1yy} \cong -1 - \frac{2}{k_0 W}\mathrm{Im}\left[T_y(\pi/2)\right] \tag{8b}$$

By using these approximate formulas (8a) and (8b), similar relations for ε_{1xy}, ε_{1yx} can be obtained from $T_x(\Phi)$, $T_y(\Phi)$ with an oblique polarization giving information for both directions. Particularly for $\Phi = \pi/4$, both components are sufficiently large and the following approximate expressions are derived:

$$\varepsilon_{1xy} \cong \frac{2}{k_0 W}\mathrm{Im}\left[T_x(0)\right] - \frac{4}{\sqrt{2}k_0 W}\mathrm{Im}\left[T_y(\pi/4)\right] \tag{9a}$$

$$\varepsilon_{1yx} \cong \frac{2}{k_0 W}\mathrm{Im}\left[T_y(\pi/2)\right] - \frac{4}{\sqrt{2}k_0 W}\mathrm{Im}\left[T_x(\pi/4)\right] \tag{9b}$$

The aforementioned simple formulas provide alternative definitions for the permittivity tensor elements of the anisotropic material and give us a physical intuition about their role. In particular, we note that the parameters ε_{1xx} and ε_{1yy} are mainly affected by the x-polarized and the y-polarized excitation respectively. Finally, the off-diagonal quantities ε_{1xy} and ε_{1yx} are derived via studying the scattering of obliquely polarized waves too.

4. INDICATIVE RESULTS

4.1. Various Permittivities

In this subsection, we study the variation of the relative error of the predictions (8a), (8b), (9a) and (9b) with respect to the elements of the permittivity matrix. The exact values of the transmission coefficients are computed from the linear system (4a). In Fig. 2(a) we show a contour plot of the average prediction error (arithmetic mean of the four absolute errors corresponding to the four unknown elements of the permittivity tensor) over a rectangular grid of the diagonal elements ε_{1xx}, ε_{1yy}. As the representation is of qualitative value only, we think that the scale indicated by color bar is not necessary. It is observed that the difference between the approximate values and the actual ones is relatively low when $\varepsilon_{1xx} \cong \varepsilon_{1yy}$ which means that the proposed method is more successful for materials with similar behavior for both directions. It is also remarkable that the maximum error (white region) is recorded when ε_{1yy} is close to zero, while minimum difference (black region) is exhibited for $\varepsilon_{1xx} \to 0$.

In Fig. 2(b) the contour plot of the average error is depicted for variable off-diagonal elements of the permittivity tensor. One can point out that for negligible ε_{1xy} and significant ε_{1yx}, the estimation error is high; on the other hand, the approximate permittivity formulas give more reliable results when $\varepsilon_{1xy} \gg \varepsilon_{1yx}$, which could be explained by the fact that $\varepsilon_{1xx} > \varepsilon_{1yy}$ in the considered example. In addition, for increasing ε_{1xy} the prediction error is decaying and the fall is more significant when ε_{1yx} gets larger. Finally, the difference is substantial and independent from ε_{1yx} with small ε_{1xy}. It can be also noted that Fig. 2(b) examines cases of $\boldsymbol{\varepsilon}_1$ with badly broken symmetry, while the real permittivity tensor should be symmetric as indicated in [12]. This is a true statement but we think that it is worth studying fictitious materials which can be constructed in the future, violating even the most fundamental principle; moreover, the diagonals of these graphs describe currently realizable cases.

4.2. Various Thicknesses

In Fig. 3 we represent the prediction error of the proposed method in db as function of the electrical thickness of the slab for each element of the permittivity tensor. We use logarithmic scale at horizontal axis for demonstration purposes. It is apparent that the difference is increasing for larger slab thickness which is sensible as the approximation (5) gets less valid. The significance of this condition is remarked by the linearly upward sloping curves in logarithmic scale. The estimation errors for

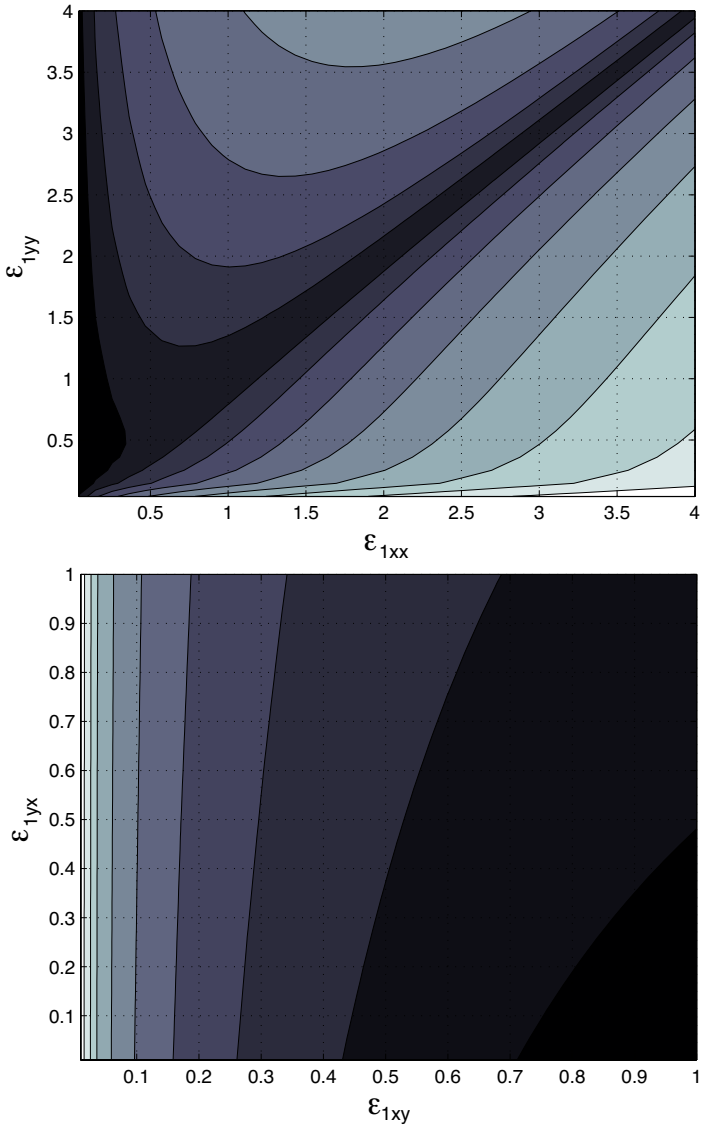

Figure 2. Contour plots of the estimation error for variable: (a) diagonal elements of the permittivity tensor with $\varepsilon_{1xy} = 0.5$, $\varepsilon_{1yx} = 0.5$, (b) off-diagonal elements of the permittivity tensor with $\varepsilon_{1xx} = 3$, $\varepsilon_{1yy} = 2$. Plot parameters: $f = 10\,\mathrm{MHz}$, $W/\lambda_0 = 10^{-4}$.

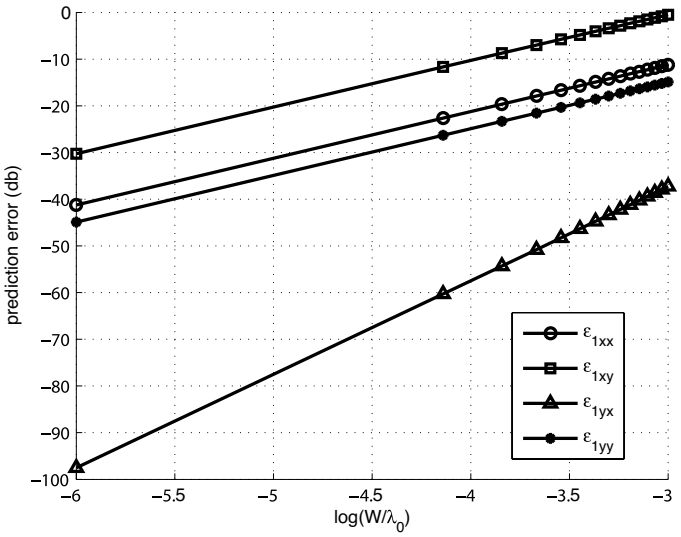

Figure 3. The prediction error for each permittivity element as function of the electrical thickness of the slab. Plot parameters: $f = 10\,\mathrm{MHz}$, $\varepsilon_{1xx} = 1.5$, $\varepsilon_{1xy} = 0.3$, $\varepsilon_{1yx} = 0.3$, $\varepsilon_{1yy} = 2.5$.

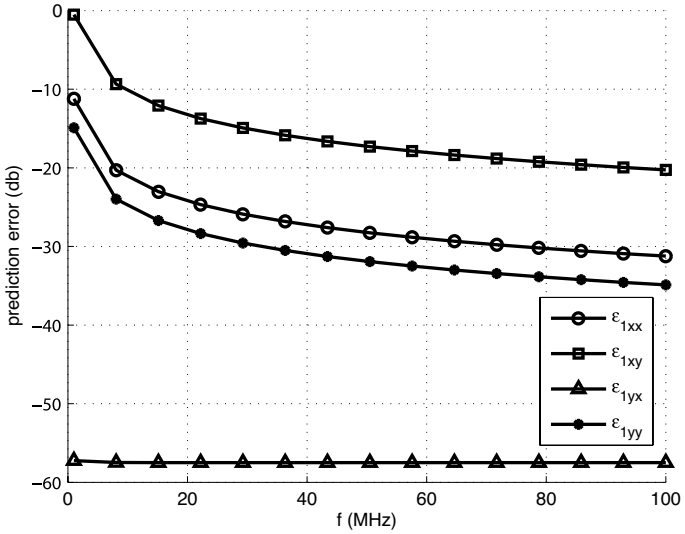

Figure 4. The prediction error for each permittivity element as function of the operating frequency. Plot parameters: $W/\lambda_0 = 10^{-4}$, $\varepsilon_{1xx} = 2$, $\varepsilon_{1xy} = 0.5$, $\varepsilon_{1yx} = 0.5$, $\varepsilon_{1yy} = 1$.

ε_{1xy}, ε_{1yx} are very different each other even though $\varepsilon_{1xy} = \varepsilon_{1yx}$ and this can be attributed to the unequal diagonal elements $\varepsilon_{1xx} \neq \varepsilon_{1yy}$. It seems that the ratio of the off-diagonal over to the corresponding diagonal element plays a pivotal role in permittivity prediction. On the other hand, the off-diagonal elements are computed with similar error although they are quite different.

4.3. Various Frequencies

In Fig. 4 we show the variation of the prediction error induced by the proposed method as function of the operating frequency with constant electrical thickness W/λ_0 of the slab. It is noteworthy that for the same electrical size the estimation errors are negatively related to the oscillation frequency and this is owed to the fact that the approximation (5) is based on small-W assumption, instead of small-k_0W one.

5. CONCLUSION

A relatively accurate measurement technique for the permittivity tensor of an electrically anisotropic material is presented. A thin slice from this substance scatters a normally incident wave of arbitrary polarization. We consider the Taylor expansion of the rigorous formulas for small slab thickness, and then simplified approximations of the permittivities are straightforwardly derived with suitably polarized excitations. The obtained expressions are both simple providing physical intuition for the dielectric constants of the material, and accurate as the transmission coefficients are easily measured.

The described method can be applied to multi-layered isotropic structures in an attempt to guess the permittivity variation along the axis of the device. In addition, the normal or oblique ray scattering by bianisotropic structures could lead to unified formulas covering a variety of interesting inverse problems of practical interest. Finally, similar results could be obtained for materials with horizontally inhomogeneous anisotropy by using Gaussian beam excitation instead of an incident plane wave.

REFERENCES

1. Gomes Neto, M. L. C., A. L. P. S. Campos, and A. G. d'Assuncao, "Scattering analysis of frequency-selective surfaces on anisotropic substrates using the Hertz vector-potential method," *Microwave and Optical Technology Letters*, Vol. 44, 67–71, 2005.

2. Valagiannopoulos, C. A., "Study of an electrically anisotropic cylinder excited magnetically by a straight strip line," *Progress In Electromagnetic Research*, PIER 73, 297–325, 2007.
3. Kokkorakis, G. C., "Scalar equations for scattering by rotationally symmetric radially inhomogeneous anisotropic sphere," *Progress In Electromagnetics Research Letters*, Vol. 3, 179–186, 2008.
4. Wang, M. Y., J. Xu, J. Wu, B. Wei, H. L. Li, T. Xu, and D. B. Ge, "FDTD study on wave propagation in layered structures with biaxial anisotropic metamaterials," *Progress In Electromagnetics Research*, PIER 81, 253–265, 2008.
5. Kukharchik, P. D., V. M. Serdyuk, and J. A. Titovitsky, "Diffraction of hybrid modes in a cylindrical cavity resonator by a transverse circular slot with a plane anisotropic dielectric layer," *Progress In Electromagnetics Research B*, Vol. 3, 73–94, 2008.
6. Chiu, C.-C. and R.-H. Yang, "Inverse scattering of biaxial cylinders," *Microwave and Optical Technology Letters*, Vol. 9, 292–302, 1995.
7. Cui, T. J., C. H. Liang, and W. Wiesbeck, "Closed-form solutions for one-dimensional inhomogeneous anisotropic medium in a special case — Part II: Inverse scattering problem," *IEEE Transactions on Antennas and Propagation*, Vol. 45, 942–948, 1997.
8. Sheen, D. and D. Shepelsky, "Inverse scattering problem for a stratified anisotropic slab," *Inverse Problem*, Vol. 15, 499–514, 1999.
9. Chen, X., T. M. Grzegorczyk, and J. A. Kong, "Optimization approach to the retrieval of the constitutive parameters of a slab of general bianisotropic medium," *Progress In Electromagnetics Research*, PIER 60, 1–18, 2006.
10. Monzon, J. C. and N. J. Damaskos, "Two-dimensional scattering by a homogeneous anisotropic rod," *IEEE Transactions on Antennas and Propagation*, Vol. 34, 1243–1249, 1986.
11. Ren, W. and X. B. Wu, "Application of an eigenfunction representation to the scattering of a plane wave by an anisotropically coated circular cylinder," *Journal of Physics D: Applied Physics*, Vol. 28, 1031–1039, 1995.
12. Born, M. and E. Wolf, *Principles of Optics*, 666, Eqn. (8), Pergamon Press, Oxford, 1968.